Using fractional condensation to optimise aqueous pyrolysis condensates for downstream microbial conversion

George Kofi Parku, Anke Krutof, Axel Funke*, Daniel Richter, Nicolaus Dahmen

Institute of Catalysis Research and Technology (IKFT), Karlsruhe Institute of Technology (KIT),
Hermann-von-Helmholtz-Platz 1, 76344 Eggenstein-Leopoldshafen,
Germany.

*Corresponding author: Email address: axel.funke@kit.edu

Abstract

This study investigates the use of fractional condensation, following the fast pyrolysis of three different ash-rich biomass feedstocks to optimise the composition of aqueous pyrolysis condensates (AC) for downstream microbial conversion. Optimum conditions were first predicted and established theoretically by means of vapour-liquid equilibrium flash calculations that employed the modified UNIFAC Dortmund (UNIFAC-DMD) model. Thereafter, theoretical models were experimentally validated on a 10 kg/h fast pyrolysis setup. Model predictions revealed that temperature combinations of 120 and 50 ^{o}C on first and second staged condensers, respectively returned optimum production of AC yield and substrates at the expense of inhibitors. Satisfactory agreement existed between most experimental data and model predictions and the qualitative trend was mostly reproduced correctly. Some noteworthy deviations were however observed, most especially for inhibitory compounds, which was blamed on the limitation of the UNIFAC-DMD model in accurately predicting the phase behaviour of organic compounds at such very low concentrations as well as the scarcity of precise vapour pressure data for some of these organic compounds. Nonetheless, the study demonstrated how valuable theoretical phase equilibria models are in predicting the composition of fast pyrolysis bio-oils and how fractional condensation proves to be a key upstream pre-treatment for valorising ACs.

Keywords: Fast pyrolysis; Thermodynamic vapour-liquid equilibrium (VLE); aqueous pyrolysis condensate, Fractional Condensation, modified UNIFAC Dortmund (UNIFAC-DMD).

1. Introduction

Projected depletion and rising carbon footprint associated with the use of fossil resources coupled with rising energy demands have sparked the production of fuels and chemicals from biomass [1,2]. Several thermal and biochemical processes have been developed to valorise biomass residues as carbon neutral resources [1,3,4]. Fast pyrolysis to convert lignocellulosic biomass into bio-based energy and chemicals has gained significant attention, due to its advantages of processing many types of biomass feedstocks into energy-dense liquid and solid intermediates for further energetic or chemical use [3,5–10]. Fast pyrolysis decomposes lignocellulosic biomass at temperatures of around 500 ^{0}C in an inert environment to produce, fast pyrolysis bio-oil (FPBO), char (containing inorganics) and non-condensable gases, each of which can be used for fuel and chemical applications [1,4,11–16]. By pyrolysis, up to 75 wt.% of initial dry biomass can be converted into FPBO [4,16]. FPBO is a complex product as a mixture of numerous compounds that include organic acids, ketones, aldehydes, alcohols, furans, phenols, hydro sugars and other oxygenates as well as water [4,14,17–20]. Due to its complex nature, FPBO may be separated into various fractions to tailor its quality for specific applications [21]. Methods employed for the fractionation of FPBO include but are not limited to centrifugation, extraction, liquid chromatography, molecular distillation and fractional condensation [4,14,22]. Centrifugation, extraction and liquid chromatography, although proven to be effective in separating FPBO, are expensive and impractical at industrial scales [2,4,14,15]. Molecular distillation is dissuaded as oxygenated compounds in the FPBO become highly reactive during heating and may polymerise into coke (solid carbonaceous residue) [1,2,4,8,12,23].

Fractional condensation to separate FPBO into useful fractions has received increasing attention [2,14,22], due to its energetic and economic advantages compared to liquid-liquid separation technologies [4,8,14]. During fractional condensation, pyrolysis vapours pass through a series of condensation stages operated at steadily decreasing temperatures, allowing for FPBO fractions of different physical and chemical properties to be collected [1,2,12,24,25]. This leads to the recovery of different phases of FPBO in the form of organic-rich (ORC) and aqueous pyrolysis condensates (AC) [18,19,26]. ORC, due to its comparatively higher calorific value has been extensively used for fuel applications. AC, however primarily comprises of up to 85 wt.% water and other organics such as carboxylic acids, furans, ketones and phenol derivatives. It has a high corrosiveness (due to the presence of the low molecular weight carboxylic acids) and very low calorific value and requires costly treatment methods to remove the organics present before being discarded in an environmentally friendly fashion [27–30]. Consequently, condensation of the aqueous phase is avoided in industrial fast pyrolysis units and the vapours are combusted along with pyrolysis gas and char to supply heat to the process.

Alternatives are being developed to utilise AC, for instance as gasifier feed after mixing with char [31,32]. Another possibility has been reported by studies on the use of this phase as a carbon source for microbial cultivation and as a substrate for anaerobic digestion [18,20,29,30,33,34]. This is due to the presence of compounds such as acetic acid in AC, which have been reported to promote microbial growth [18,29,35].

A major setback commonly encountered in cultivating microbes on AC is the elimination of potential growth inhibitors (furans, ketones and some phenol derivatives) from AC to tailor its use as substrate [20,27,30,35]. Several techniques to curtail these have been investigated, including liquid-liquid extraction [16], adsorption using pyrolysis char as activated carbon [30,36], rotary evaporation [20,35] and overliming [29,35,37–39]. In as much as these techniques tend to be promising, the majority of them require separate downstream processes in addition to the fast pyrolysis process. This will most likely impact economic feasibility towards attaining a sustainable biorefinery concept as was concluded in the studies of Liaw et al. [33].

Removal of inhibitory compounds from the AC using optimised fractional condensation may lead to a novel growth medium for microbial cultivation. Liaw et al. [33] adjusted the temperature of only the first stage in a fractional condensation setup to study the composition of the produced phases, but no study has been found where the temperatures of all stages are independent variables. In fractional condensation, temperature adjustment of each condensation stage is essential to optimising the composition of AC for its use as substrate.

A relevant challenge met when modelling fast pyrolysis, including the condensation of fast pyrolysis volatiles, is the physicochemical characterisation of the compounds found in the model [13,40,41]. Westerhof et al. [42] demonstrated this when they predicted the effects of condensation conditions on fractions of light compounds using a simple equilibrium stage model. Westerhof et al. [43] also previously compared an equilibrium flash condensation model with experimental results when they studied the control of water content in FPBO.

The ability to model condensation systems using simple flash abstractions allows the study of separation systems without the time and effort required to perform these studies in a real setup. Modelling the vapour-liquid equilibrium (VLE) requires the user to choose a thermodynamic model, and Carlson [44] recommends the use of activity coefficient models to model mixtures rich in non-ideal components. Many of the components of pyrolysis condensates lack model parameters in databases or in the literature, therefore the use of group-contribution models, such as modified UNIFAC Dortmund (UNIFAC-DMD) [13] and the Group Contribution with Association Equation of State (GCA-EoS) [40] is favourable. Both models have been reported to be reliable tools to predict phase equilibria (including FPBO condensation processes) over wide temperature ranges and have seen numerous applications in research and industry [13,40,41,45,46].

This study aims to optimise the composition of an aqueous condensate (AC) obtained from fractional condensation of fast pyrolysis vapours within the bioliq® concept of biomass fast pyrolysis [24,47] of three ash-rich biomass feedstocks (wheat straw, *miscanthus* and coffee husk) for downstream microbial conversion. Theoretical studies of two condensation steps with a UNIFAC-DMD thermodynamic model were conducted. Central Composite Design (CCD) methodologies were applied to estimate an optimum combination of the two condensation temperatures to maximise the concentration of substrates and the yield of the desired product, as well as minimise the concentration of inhibitors. The obtained optimum condensation setup was tested in a 10 kg/h fast pyrolysis pilot unit. The unique combination of applying a proven thermodynamic model with experimental validation of the calculated results represents a decisive addition to previous studies in the field of AC valorisation and condensation of FPBOs.

2. Materials and Methods

The study employed the fast pyrolysis of three ash-rich biomass feedstocks. These are wheat straw, coffee husk (residues from agriculture) and *miscanthus* (a perennial grass) available in large quantities. These raw materials were chosen because they contain a high amount of minerals, especially potassium. Like most alkali (earth) metals, potassium is known to catalyse pyrolysis reactions, which in consequence leads to increased formation of char and reaction water during fast pyrolysis [24,25]. Consequently, fractionated condensation becomes more important in this case.

Wheat straw was supplied by Franz Kolb GmbH & Co. KG, Germany (firma-kolb.de) and was shredded in batches of two bales of 200 kg (April 2019) and 300 – 400 kg (December 2020). The batch shredded in April 2019 was used for generating initial AC used for tolerance tests of microbes (section 2.1.1) whereas the batch shredded in December 2020 was used for validation experiments following model predictions (section 2.2). Prior to the experiments, wheat straw was shredded using a shredder (HZR 1300) and subsequently milled using a cutting mill (TYP LM 450/1000-S5-2) to particle sizes below 5 mm. Both equipment were supplied and installed by Neue Herbold Maschinen- und Anlagenbau GmbH (Sinsheim, Germany).

Miscanthus was supplied by Miscanthus Falzberger, Pichl bei Wels, Austria in large bales of about 500 kg each. The batch was harvested in April 2020. Particle size reduction of *miscanthus* followed the same procedure used for wheat straw to generate final particle sizes of 5 mm and below.

Colombian coffee husk was supplied by the Universidad Nacional de Colombia, Sede Medellín. The feedstock was originally obtained from "*ALMAVIVA*", a logistic centre for the

National Federation of Coffee Growers in Medellin, Colombia. The batch was harvested in July 2019. Maximum and minimum chord lengths of coffee husk for 90% of the particles were less than 7.5 mm and 4.2 mm, respectively, with particle thickness ranging between 0.1 mm and 0.2 mm. Coffee husk did not require any further size reduction before pyrolysis.

2.1. Modelling optimisation of the fractional condensation process

2.1.1 Selection of surrogate/model mixtures for thermodynamic VLE modelling

A surrogate mixture for the AC was designed following GC-MS analysis of a sample obtained from the fast pyrolysis of wheat straw on a 10 kg/h process development unit (PDU) (described in detail in section 2.2) and tolerance and toxicity tests for microbes on this sample. This followed similar procedure employed elsewhere [19]. Toxicity and tolerance tests were conducted to investigate how much and to what extent microbes are able to tolerate compounds present in a particular substrate such as AC. For example, following toxicity testing, it was confirmed that compounds such as acetic acid and acetol are good substrates that aid the growth of microbes, whereas compounds such as furfural have been identified to inhibit microbial growth.

The selection procedure of surrogate components followed a similar principle as the one employed by Ille et al. [13], ensuring compounds of interest to microbial conversion (as both substrates and inhibitors) were included. Generally, the following factors were considered:

1. Representation of the surrogate mixtures such that they cover the whole boiling point range of the individual components present in AC.
2. Representation of all relevant functional groups in the original AC mixture.
3. Interest of compounds to microbial conversion.

4. Mass fraction (wt.%) of the chosen compound.

The selection of surrogate compounds based on the overall GC-MS characterisation of the AC and toxicity testing of microbes has been presented in detail in Section A of supplementary information. A similar procedure was also employed in defining surrogate mixtures for *miscanthus* and coffee husk. Generated model compounds for all three biomass feedstocks were categorised into substrates and inhibitors and have been summarised in Table 1.

The mass fractions (in wt.%) of selected surrogate compounds in pyrolysis vapours entering the first condensation unit were estimated using their corresponding mass fractions in the ORCs and ACs, as well as stream flow rates of the condensation setup. GC-undetectable lignin-derived components present in ORC were represented as 3,4,4'-Biphenoltriol, as was similarly implemented by Ille et al. [13]. Consequently, these estimated mass fractions served as input stream mass fractions for thermodynamic VLE flash calculations (section 2.1.3). The resulting surrogate mixtures with their respective mass fractions (in pyrolysis vapours entering the first condensation unit) for all three biomasses and the GC-MS data for all AC and ORC samples for all three biomass feedstocks have been presented in Tables S4 and Tables S9 - S14, respectively in section C of supplementary information.

Yields of ORC (Y_{ORC}) and AC (Y_{AC}) were estimated with respect to the total input vapour flow into the first condenser ($m_{tot\ vapours\ into\ C1}$), defined by Eqs. (1) and (2).

$$Y_{ORC} = \frac{m_{ORC}}{m_{tot\ vapours\ into\ C1}} \qquad (1)$$

$$Y_{AC} = \frac{m_{AC}}{m_{tot\ vapours\ into\ C1}} \qquad (2)$$

Table 1. Grouping of surrogate/model compounds of AC into substrates and inhibitors for all three biomass feedstocks.

Substrates/Promoters	**Inhibitors**
Hydroxyacetaldehyde	3-hydroxy-propionaldehyde
Acetic Acid	2-Butanone
Propionic Acid	Methanol
Acetol	Furfural
Phenol	O-Cresol
Ethylene Glycol	M-Cresol
Guaiacol	Syringol
2-methyl-propanoic acid	5-hydroxymethyl-2-furaldehyde
	Vanillin
	2,3-Butandione (Diacetyl)
	1-hydroxy-2-butanone

2.1.2 Central composite Design (CCD)

A Central Composite Design (CCD) statistical method with five centre points was used to ascertain the optimal temperature conditions at which the production of substrates supersedes inhibitors. Design Expert software, version 12 (Stat-Ease Inc., Minneapolis, USA) was used for setting up the design and evaluation of the CCD. Temperatures of Condensers 1 (C1) and 2 (C2) were the factors investigated whereas mass fractions of substrates and inhibitory compounds (in wt.%) recovered in AC, yield of the AC, ratio of substrates to inhibitors and mass fraction of water in AC were the main response variables. The temperature ranges of C1 and C2 investigated were 80 – 120 ^{o}C and 10 – 50 ^{o}C, respectively. These ranges were chosen considering the operability ranges of the condensers, as well as avoiding operating temperatures below 80 ^{o}C on C1 (conditions that facilitate the recovery of 2-phase liquid products). Also, for C2, operating this unit above 50 ^{o}C leads to significant loss of aqueous condensate products. Factors under scrutiny and their operating ranges as designed using the CCD have been presented in Table S5 in section B of supplementary information.

2.1.3 Thermodynamic VLE flash calculations

Following the design of temperature ranges to be investigated using the CCD, thermodynamic VLE flash calculations were performed using the UNIFAC-DMD thermodynamic model. The UNIFAC-DMD model was programmed in MATLAB using the latest database obtained from the UNIFAC Consortium from Dortmund Data Bank [48]. Thermodynamic VLE calculations were performed around the condensation unit of the fast pyrolysis PDU described in section 2.2 and depicted in Fig. 1, in which units 5 and 9 represent the first and second condensers to produce ORC and AC, respectively. It is important to note that aerosols formed during first cooling in the first condensation stage were recovered in an electrostatic precipitator and added to the ORC. Consequently, it is feasible to represent each condenser with flash calculations. Flash calculations were performed using temperature pairs of C1 and C2 that were defined from the CCD (Tables S6 to S8 in section B of supplementary information) to obtain corresponding data of response factors.

The generalised laws of Raoult and Dalton (Eq. (*3*) form the basis for modelling typical G^E models like the UNIFAC-DMD. VLE flash calculations were formulated using this relation. Where, x_i and y_i represent the mass fractions of pure components in the liquid and vapour phases, respectively. P and P_i^0, the total pressure and the pure substance saturated vapour pressure, respectively. The poynting correction, Φ_i defines the vapour-phase non-ideality with the activity coefficient, γ_i accounting for liquid-phase deviation from ideal solution behaviour. It is important to note that the poynting correction for high pressures was approximated to unity in this study since the condensation process was at atmospheric pressure.

$$y_i \Phi_i P = x_i \gamma_i P_i^0 \tag{3}$$

The saturated vapour pressure of pure substances, P_i^0 were defined using the Wagner equation (Eq. (*4*)[49–51].

$$\ln \frac{P_i^0}{P_c} = \frac{1}{T_r}\left[A(1-T_r) + B(1-T_r)^{1.5} + C(1-T_r)^{2.5} + D(1-T_r)^5\right] \tag{4}$$

$$T_r = T/T_c \tag{5}$$

P_c and T_r represent the critical pressure and reduced temperature, respectively. T_r (Eq. (5), is a function of the thermodynamic temperature, T and the critical temperature, T_c. The constants A, B, C and D are the Wagner constants. The Wagner constants for majority of the compounds were obtained elsewhere [51,52]. Wagner constants for all other substances were estimated using the Extended Antoine Equation from Aspen Plus physical property system pure component databank.

2.2. Experimental validations on Process Development Unit (PDU)

Subsequent to the modelling optimisation study, optimum condensation temperatures were experimentally validated on a 10 kg/h pyrolysis PDU, a scaled-down version of the bioliq® process. A detailed process description of this unit has been elaborated elsewhere [53,54], thus only a brief description of modifications made have been provided here. An overview of the setup has been depicted in Fig. 1.

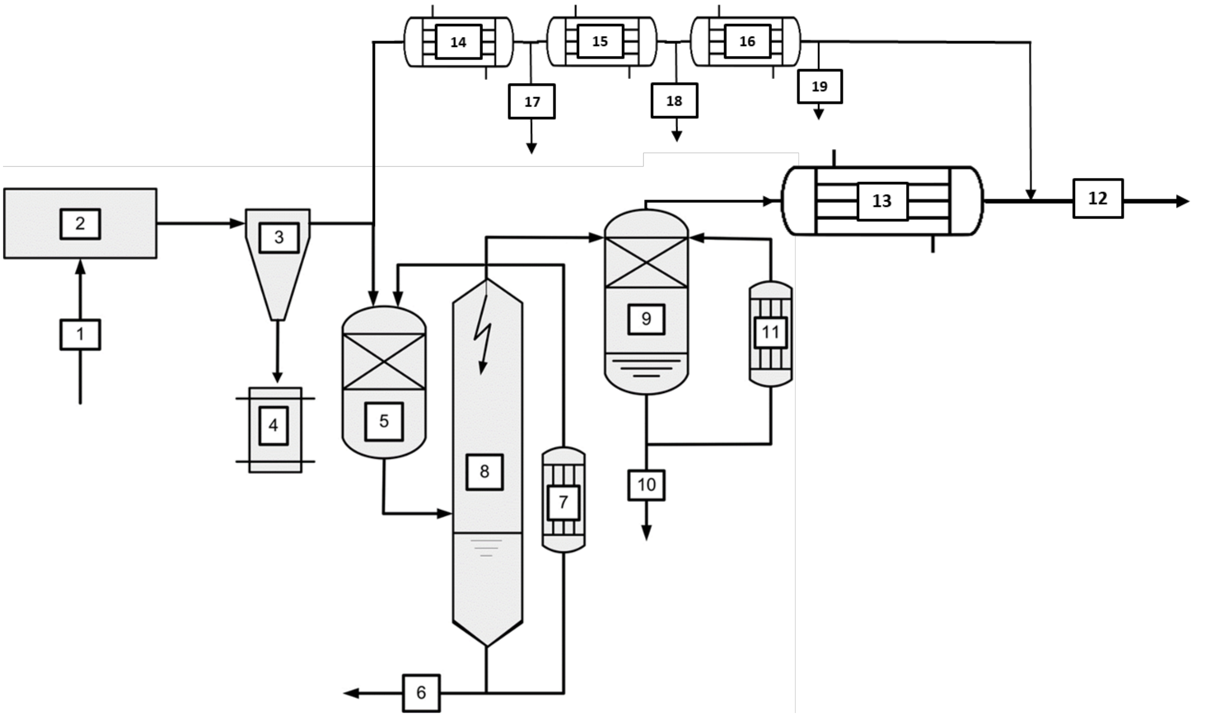

Fig. 1. Schematic of the fast pyrolysis Process Development unit (PDU): 1: Biomass Feed, 2: Pyrolysis screw reactor, 3: Cyclone, 4: Solid char products, 5: Quenching Condenser 1, 6: Organic rich condensate (ORC), 7: Heat exchanger 1, 8: Electrostatic precipitator, 9: Quenching Condenser 2, 10: Aqueous condensate (AC), 11: Heat exchanger 2, 12: Incondensable gases, 13: Third condensation

unit, 14: Bypass condenser 1, 15: Bypass condenser 2, 16: Bypass condenser 3, 17: ORC from bypass, 18: AC1 from bypass, 19: AC2 from bypass. (Adapted from Ille et al. [13] with permission from Elsevier*)*

Validating the optimised temperature conditions from the CCD investigation mandated a modification of the PDU condensation setup since it was not initially designed to operate at these optimised condensation temperatures. These modifications included a third condensation unit designed as a shell-and-tube condenser that also operated at temperature conditions similar to C2 with the sole purpose of recovering any AC which could not condense in C2 as a result of a higher operating temperature (50 ^{o}C) as compared to the default/conventional operating temperature (15 ^{o}C). All experiments were conducted in triplicates to ensure reproducibility.

Due to the fact that ORC and AC obtained from these main condensation loops are heavily diluted with the quenching liquids, ethylene glycol and water respectively, a bypass condensation loop (units 14, 15 and 16 of Fig. 1) was installed and attached to the PDU to recover undiluted pyrolysis oil products. The bypass condensation loops are shell and tube condensers with operating temperature conditions similar to the main quenching condensation loops. These undiluted pyrolysis products provide a more accurate representation of the pyrolysis condensates hence their GC-MS characterisation results were used (for experimental validation) instead of the GC-MS characterisation of the heavily diluted samples.

2.3. Analytic methods

For every test conducted on the PDU, biomass samples, solid char and all condensates were subjected to various analyses. The methods followed similar procedures employed elsewhere [54] with only summaries being highlighted here.

The moisture content of biomass feedstocks and char was measured in accordance with DIN EN 18134-3. Volumetric Karl-Fischer titration was done using methanol with Hydranal Composite-V to determine water content in all condensates. Ash content of biomass feedstocks and solid char was conducted per DIN EN ISO 18122, where samples were heated to 250 ^{0}C for 60 min, and subsequently to 550 ^{0}C for 120 min. Volatile matter of biomass feedstocks were conducted following DIN EN ISO 18123. Elemental analysis for solid char was according to DIN EN 15104 and DIN EN 51732 for biomass feedstocks and ORCs.

The composition of non-condensable gases was characterised online using gas chromatography with neon gas as a tracer. Gas volumetric flowrate was additionally measured using an online flowmeter.

GC–MS analyses of all pyrolysis condensates were conducted by the Thünen Institute, Hamburg, Germany. The method has been described in detail elsewhere [55].

3. Results and Discussions

3.1. Modelling optimisation of the fractional condensation process

The two-unit condensation setup (described in section 2.2) was modelled to determine the effects of their operating temperatures on variation in mass fractions of substrates and inhibitor compounds in the recovered AC. Temperature ranges of 80 and 120 ^{0}C were investigated for the first condenser whereas ranges of 10 and 50 ^{0}C were considered for the second condenser.

The influence of condenser temperatures on the mass fractions of substrate and inhibitor compounds (based on selected surrogate mixtures shown in Table 1) present in AC were evaluated. Additionally, ratio parameters of substrate to inhibitor compounds was used to further buttress conditions at which recovery of substrates were optimum. Furthermore, the effects of temperature variation on yields and water content of the AC were also investigated. The investigation was done for three different biomass feedstocks: wheat straw, *miscanthus* and coffee husk.

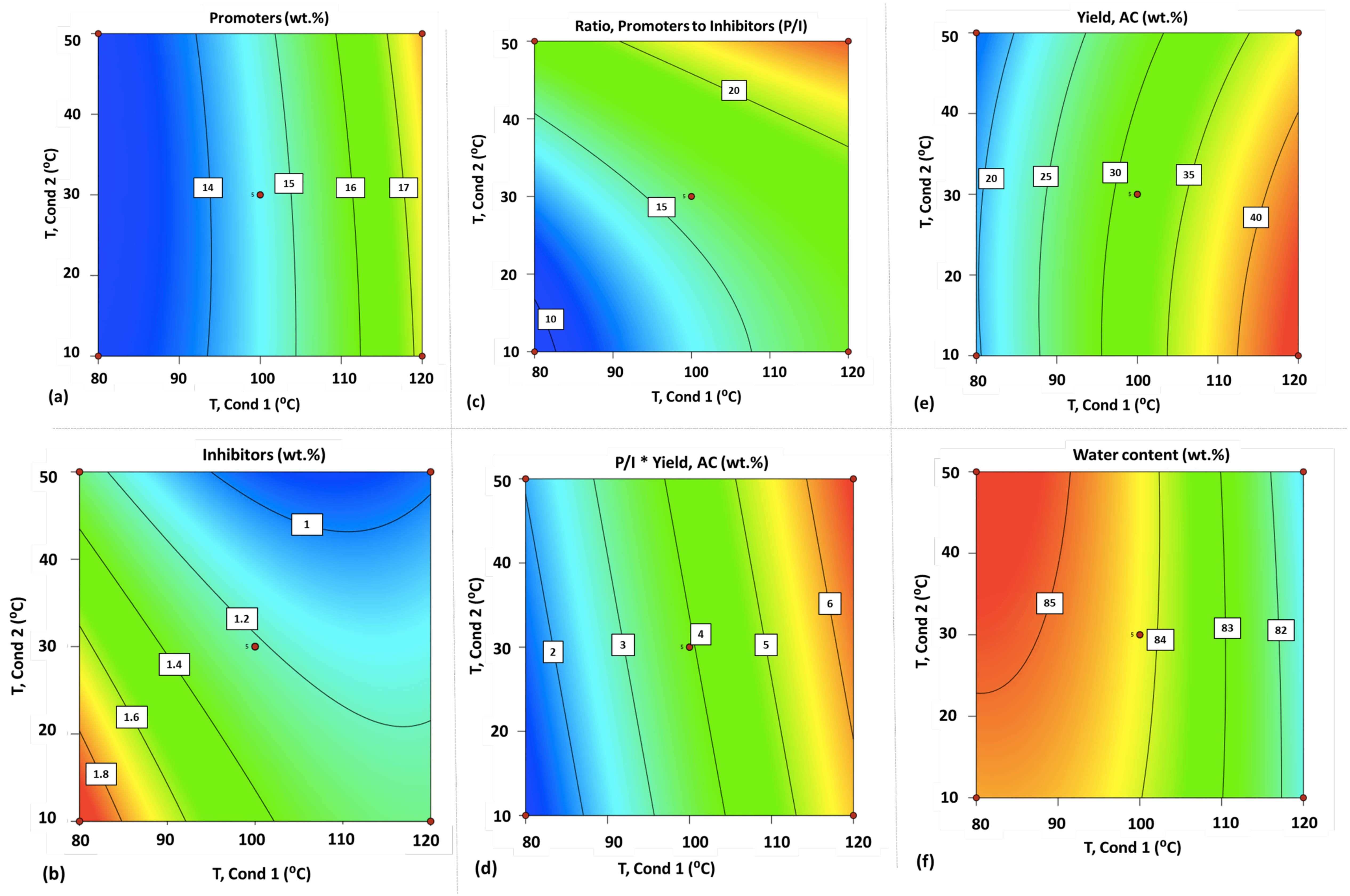

*Fig. 2. Wheat Straw: Effects of condensation temperatures on: (a) Mass fraction of the sum of promoter/substrate compounds in AC; (b) Mass fraction of the sum of inhibitory compounds in AC; (c) Ratio of promoters (P) to inhibitors (I): (d) proportion ratio of promoters to inhibitors with respect to AC yield; (e) AC yield (based on the vapour flow at the inlet of the first condenser); and (f) water content in AC. *Cond-Condenser*

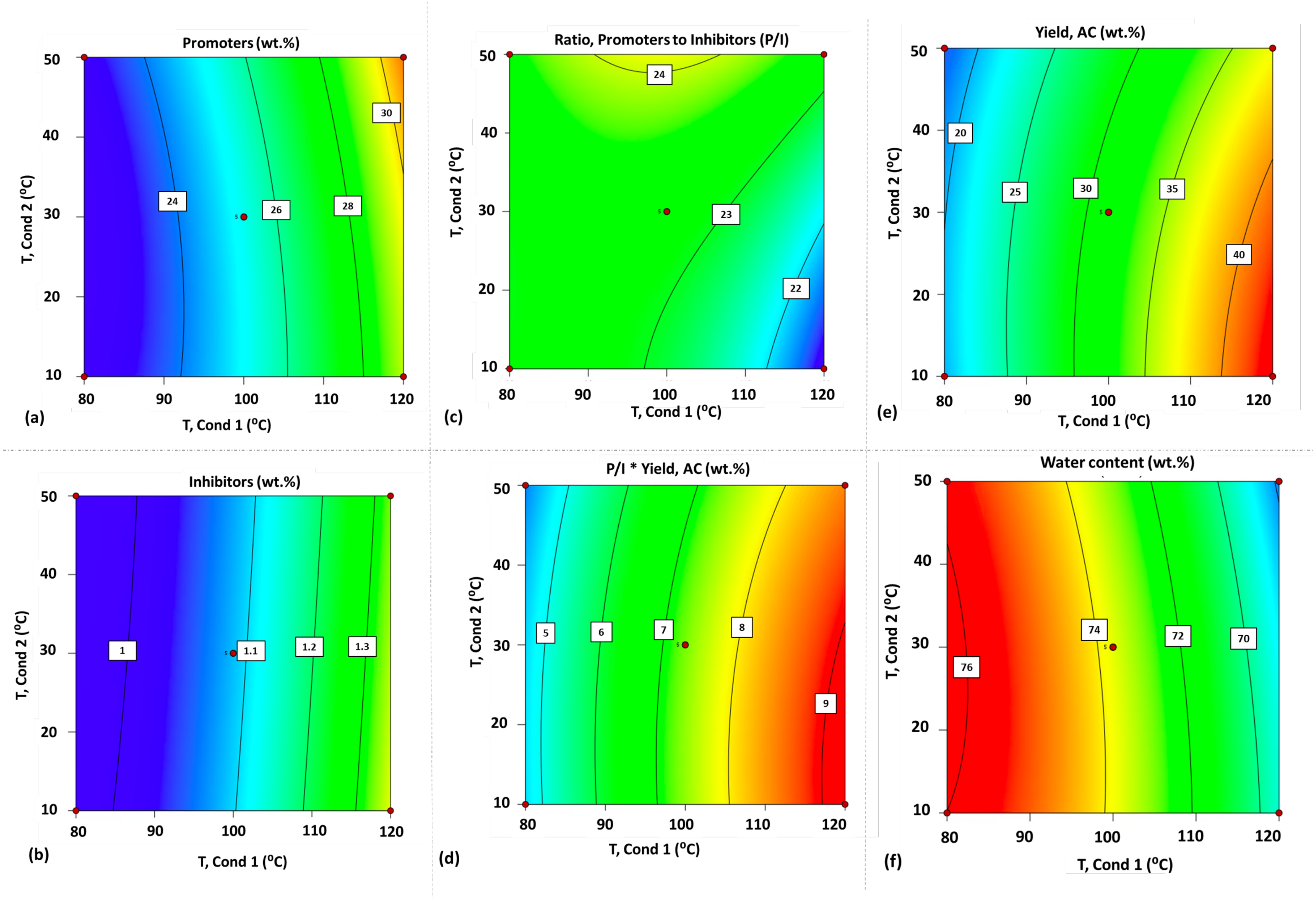

*Fig. 3. Miscanthus: Effects of condensation temperatures on: (a) Mass fraction of the sum of promoter/substrate compounds in AC; (b) Mass fraction of the sum of inhibitory compounds in AC; (c) Ratio of promoters (P) to inhibitors (I): (d) proportion ratio of promoters to inhibitors with respect to AC yield; (e) AC yield (based on the vapour flow at the inlet of the first condenser); and (f) water content in AC. *Cond-Condenser*

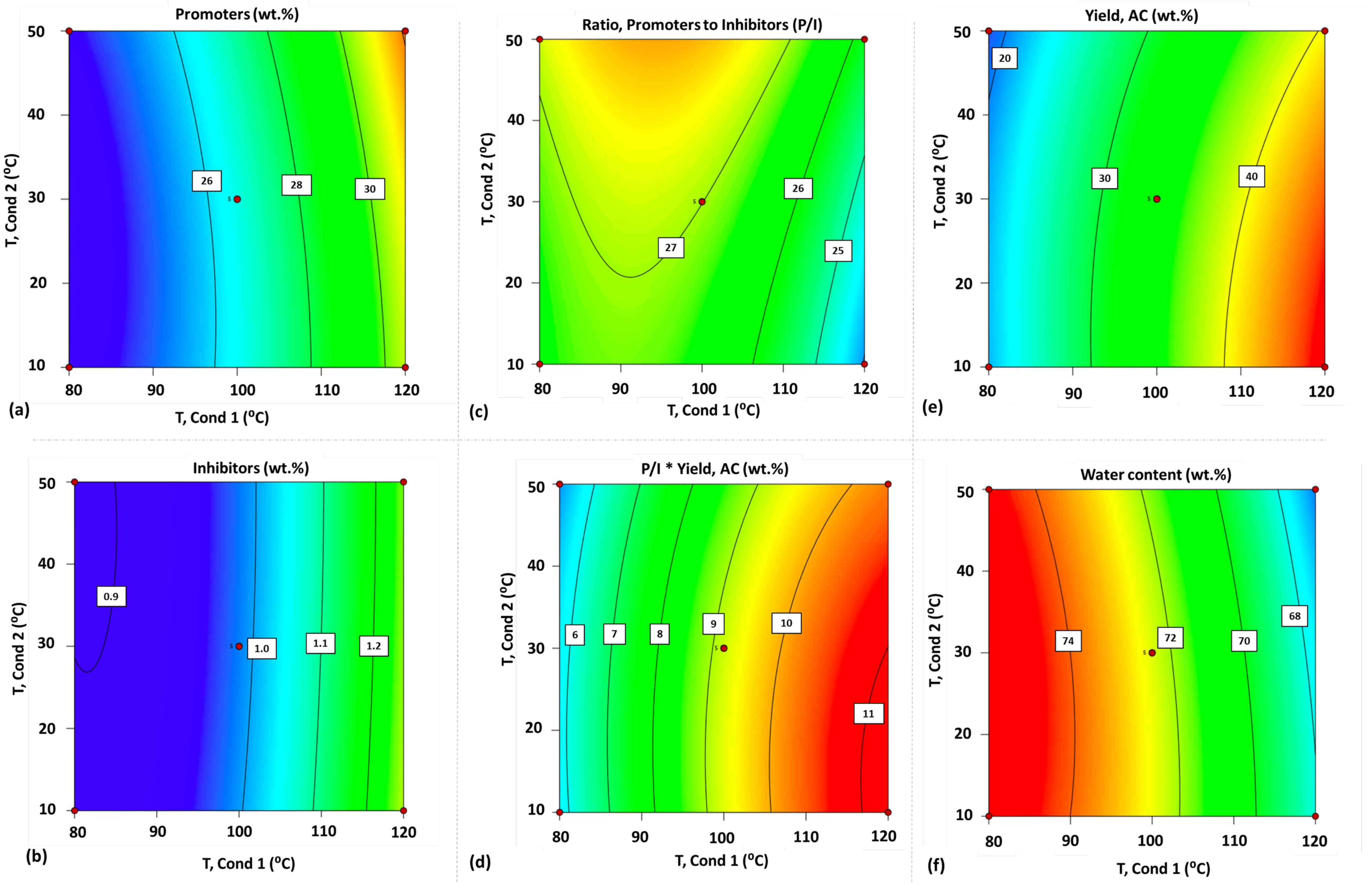

*Fig. 4. Coffee Husk: Effects of condensation temperatures on: (a) Mass fraction of the sum of promoter/substrate compounds in AC; (b) Mass fraction of the sum of inhibitory compounds in AC; (c) Ratio of promoters (P) to inhibitors (I): (d) proportion ratio of promoters to inhibitors with respect to AC yield; (e) AC yield (based on the vapour flow at the inlet of the first condenser); and (f) water content in AC. *Cond-Condenser*

3.1.1 Wheat Straw

In Fig. 2a, it was observed that increasing the temperature of the first condenser from 80 to 120 ^{o}C had the greatest effect on the recovery of substrates in AC, with substrate mass fraction increasing from about 13 to 18 wt.%. This increase is because at higher temperatures, more substrate compounds (especially acetic acid, propionic acid and acetol) remain in the vapour phase in the first condenser and are only condensed in the AC in the next stage. Similar observations were made by Liaw et al. [33] who also observed an increase in the mass fraction of compounds such as acetic acid and acetol in their AC when temperature of the first staged condenser increased. Generally, the influence of temperature in the second stage condenser on the mass fraction of substrates in AC was seen to be insignificant. At lower temperatures of C1 (80 ^{o}C), virtually no change in the mass fraction of substrates were observed when the temperature of C2 rose from 10 to 50 ^{o}C. Also, for the same temperature range of C2, only a slight increase (about 0.5 wt.%) in the mass fraction was observed at a higher operating condition of C1 (120 ^{o}C). The highest yield of substrate (about 18 wt.%) was recorded at a temperature combination of 120 ^{o}C and 50 ^{o}C on C1 and C2, respectively.

From Fig. 2b, throughout the temperature range of C1 (80 – 120 ^{o}C), a decrease in the mass fraction of inhibitors was observed when the temperature of C2 rose from 10 to 50 ^{o}C. Decreases from 1.98 to 1.28 wt.% (at C1 temperature of 80 ^{o}C) and from 1.26 to 0.98 wt.% (at C1 temperature of 120 ^{o}C) were observed. The lowest mass fraction of inhibitors (about 0.98 wt.%) was recorded at the highest operating temperature combinations of both condensers as these conditions fostered the condensation of most of the higher molecular weight compounds that include furfural, syringol, m-Cresol and o-Cresol (which form the majority fraction of inhibitors) in the first condensation stage. Due to their comparatively higher boiling points, they tend to be retained at higher operating temperatures of C1, which will mean only significantly lower fractions of these components progress to the next condensation stage. It is also important to mention that at higher operating temperatures of both condensers, the inhibitor methanol remains in its vapour phase, implying that its concentration level in the recovered AC is below thresholds that can cause toxicity.

To get a clearer picture of the recovery of substrates/promoters (P) and inhibitory (I) compounds in AC, the ratio of their respective mass fractions was multiplied by the yield of AC to generate the parameter, "P/I * Yield of AC". This parameter ascertained the fact that an increase in temperature on both condensation units facilitated the production of substrates to the detriment of inhibitors at an optimal recovery of AC, as can be seen in Fig. 2d. Proportions of inhibitors were suppressed about six folds when operating temperatures of both condensers increased from the lowest to highest. Even more conspicuous with this trend is the direct ratio of promoters to inhibitors (Ratio, P/I) (Fig. 2c), which saw an exponential rise from about 10 to 25 as the temperatures of both condensation stages increased from their lowest to their highest ranges investigated.

From Fig. 2e, the yield of AC (with reference to the input vapour flow in the first condenser) is greatly influenced by temperature change in the first condenser. By increasing the temperature on the first condenser from 80 to 120 ^{o}C, an increase in the yield of AC from about 18 wt.% to a yield range of 35 – 45 wt.% was observed. This is obvious as higher temperatures on this unit would not be conducive for the condensation of water (whose boiling point is 100 ^{o}C) and hence are mostly passed on and recovered in the second condensation stage. Westerhof et al. [42] made similar observations when they varied C1 temperatures between 20 and 81 ^{o}C and recorded a gradual increase in the yield of their AC at different biomass pyrolysis temperatures. Increasing the temperature in the second condensation stage had a comparatively weaker influence on AC yield. At a fixed temperature of 120 ^{o}C in the first condenser, the yield decreased from approximately 45 to 35 wt.%, with an increase in the temperature in the second condenser from 10 to 50 ^{o}C. At a fixed temperature of 80 ^{o}C in the first condenser, hardly any change in AC yield was observed as the temperature in the second staged condenser increased (Fig. 2e).

In Fig. 2f, the influence of the temperature in the second staged condenser was also seen not to be very significant on the mass fraction of water (water content) in AC. Nonetheless, with an increase of temperature in the first condenser, the water content slightly decreased from approximately 85 to 80 wt.%.

The observed trends for all parameters discussed suggested that for the temperature ranges investigated, combinations of 120 ^{o}C (on the first staged condenser) and 50 ^{o}C (on the second staged condenser) returned optimum conditions for which the recovery of substrates and inhibitory compounds were at the maximum and minimum, respectively. Optimum recovery of the yield of AC was also recorded at these conditions.

3.1.2 Miscanthus and coffee husk

Like wheat straw, similar trends to the evolution of substrates with temperature rise on both condensers were observed for the cases where *miscanthus* and coffee husk were used as biomass feedstock. The highest substrate mass fraction (about 31 and 32 wt.% respectively for *miscanthus* and coffee husk) was recorded at temperature combinations of 120 ^{o}C and 50 ^{o}C, respectively on the first and second condensers. It is interesting to note that corresponding mass fractions of substrates were about twice as high in ACs recovered from *miscanthus* and coffee husk compared to ACs recovered from wheat straw. This was corroborated to the significantly higher amounts of carboxylic acids such as acetic and propionic acids (which constitute the majority fraction of substrate compounds) originally present in the volatiles generated following the pyrolysis conversion of these feedstocks (Table S4 in supplementary information). As can be seen from Table S4, the mass fractions of acetic and propionic acid originally present in the volatiles generated from the fast pyrolysis of *miscanthus* and coffee husk were about twice as high as those recorded from wheat straw pyrolysis. This could also suggest that some similarities exist in the chemical compositions and degradation mechanisms of *miscanthus* and coffee husk.

Unlike the case of wheat straw, where a decrease in the mass fraction of inhibitors was observed when condensation temperatures increased, the mass fraction of inhibitors in AC recovered from both *miscanthus* and coffee husk unexpectedly increased. An increase in yield of about 0.38 and 0.37 wt.% for *miscanthus* (Fig. 3b) and coffee husk (Fig. 4b) were obtained, respectively when temperature of C1 rose from 80 to 120 ^{o}C. Nonetheless, an increase in temperature of C2 had no significant effects on mass fractions of inhibitors. Again, in contrast to wheat straw, the lowest mass fractions of inhibitors were recorded at temperature combinations of 80 and 10 ^{o}C for C1 and C2, respectively for both feedstocks. The reason for the contradicting trends observed for *miscanthus* and coffee husk as compared to wheat straw was a result of the varying compositions of the inhibitor, 3-hydroxy-propionaldehyde in the pyrolysis volatiles of these biomasses (Table S4 of supplementary information). This strong inhibitor was only available in negligible amounts of the wheat straw pyrolysis volatiles and was hardly detected in its subsequently recovered AC product. Its composition in volatiles of *miscanthus* and coffee husk was however fairly significant and was seen to increase in AC with temperature rise of C1 although only at lower temperatures of C2 in the investigated range. It was also noted that mass fractions of other inhibitory compounds such as vanillin and furfural were at least three times higher in the pyrolysis volatiles of *miscanthus* and coffee husk than the volatiles of wheat straw (Table S4 of supplementary information).

In effect, the evolution of the ratio of substrates (promoters) to inhibitors (Ratio, P/I) with temperature rise on both condensers observed for wheat straw followed a different pattern from that observed for *miscanthus* and coffee husk. Dissimilar to wheat straw, where this parameter increased with temperature rise and peaked at C1/C2 temperature combinations of 120^{o} C/50 ^{o}C, this parameter first increased as temperatures of both C1 and C2 increased, peaked at C1/C2 temperature combinations of 100 ^{o}C/50 ^{o}C (for *miscanthus*) (Fig. 3c) and about 95 ^{o}C/50 ^{o}C (for coffee husk) (Fig. 4c), after which it decreased with subsequent increase of temperature. This corroborates the fact that inhibitory compounds became somewhat pronounced at higher condensation temperatures for *miscanthus* and coffee husk unlike the case of wheat straw, where the mass fractions of inhibitors were suppressed at an increased operating temperature of both condensers.

Yields of AC and water content for *miscanthus* (Fig. 3e & f) and coffee husk (Fig. 4e & f) followed similar trends observed for wheat straw except that water content was about 10 wt.% lower than all corresponding temperature conditions of wheat straw. This is expected as the water content originally present in wheat straw volatiles is higher than *miscanthus* and coffee husk (Table S4 of supplementary information). Another observation that further ascertains similarities in composition and degradation mechanisms of *miscanthus* and coffee husk.

Far apart from the case of wheat straw where optimum operating conditions for generating peak yields of AC and substrates at the expense of inhibitors were all slated at a single temperature combination of C1 and C2 (i.e. 120 ^{o}C/50 ^{o}C) (Fig. 2d), the instance for *miscanthus* and coffee husk were quite indistinct (Fig. 3d & Fig. 4d). Although, recommended temperature combinations for the optimum production of substrates at the expense of inhibitors were recorded at 100 ^{o}C/50 ^{o}C (for *miscanthus*) and about 95 ^{o}C/50 ^{o}C (for coffee husk), the AC recovered at these conditions was not at its apex. The optimum yields of AC for these feedstocks were only realised at C1/C2 temperature combinations of 120 ^{o}C /10 ^{o}C (Fig. 3e & Fig. 4e). However, at this temperature combination, mass fractions of inhibitory compounds were at their highest. Nonetheless, the C1/C2 temperature combination of 120 ^{o}C/50 ^{o}C appears to be the best point of compromise, as significantly higher amounts of substrates as opposed to inhibitors (1-2.5 units bereft of optimum values recorded in Fig. 3c & Fig. 4c) and AC yields of just about 5-6 wt.% short of optimum figures were still produced.

It is however important to highlight that the ORC is the main product of the fast pyrolysis process, whereas AC, a side stream. At the recommended optimum operating conditions for the valorisation of substrates from AC, the yield of the main product (ORC) becomes lower compared to normal operating conditions. As presented in Table 2, the yield of ORC for wheat straw, *miscanthus* and coffee husk decreased by 23, 15 and 17%, respectively when C1 temperature increased from conventional (90 ^{o}C) to optimum (120 ^{o}C). This development will most likely alter temperature conditions that will favour economic feasibility of the new concept (valorising AC and simultaneously recovering viable amounts of ORC). Nonetheless, very little changes are observed with the overall energy recovered with the ORC at higher condensation temperature (i.e. most differences in yield are attributed to less water content in the ORC).

Table 2. Yields of ORC obtained at conventional (90 ^{o}C) and optimum (120 ^{o}C) operating conditions of C1, highlighting the resulting percentage decreases for all three biomass feedstocks.

	ORC yield (wt.%)		
C1 Temperature (^{O}C)	Wheat Straw	*Miscanthus*	Coffee husk
90 (conventional)	60	65	65
120 (optimum)	46	55	54
Percentage decrease	23.3	15.4	16.9

*Percentage decrease represents decrease in ORC yield as temperatures increased from conventional to optimised conditions.

3.2. Experimental validations of theoretical models on a 10 kg/h PDU

3.2.1 Comparison of experimental data and model predictions for yields of substrates, inhibitors, AC yield and water content

Recommended optimum conditions (120 ^{o}C on staged condenser 1 and 50 ^{o}C on staged condenser 2) obtained from modelling study were implemented on a 10 kg/h pyrolysis PDU (earlier described in section 2.2) to validate the model prediction for all three biomass feedstocks. Subsequently, comparisons of the performance of the model predictions to experimental data were also done at conventional condensation temperature conditions of the PDU (90 ^{o}C on staged condenser 1 and 15 ^{o}C on staged condenser 2) and were compared to the recommended optimum conditions for wheat straw and *miscanthus* biomass feedstocks (Fig. 5, Fig. 6a & b). Comparisons of model predictions with experimental data for coffee husk biomass feedstock were made for recommended optimum temperature combinations only, as per experimental data available (Fig. 6c).

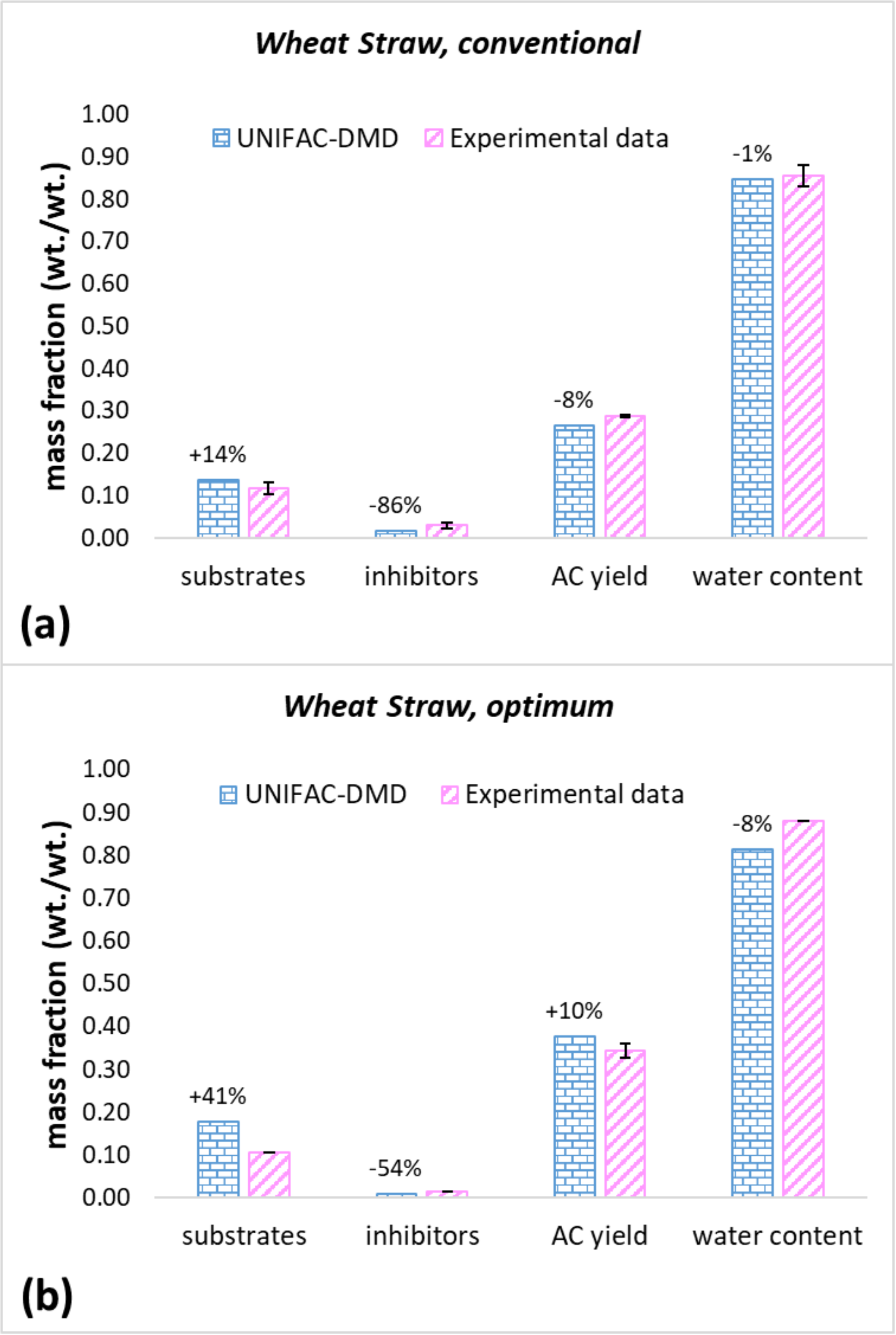

Fig. 5. Comparison of theoretical UNIFAC-DMD models for investigated parameters with experimental validations on PDU for wheat straw pyrolysis showing percentage deviations from experimental data: (a) comparisons at conventional condensation temperatures (C1-90 ^oC/C2-15 ^oC) and (b) comparisons at optimum condensation temperatures (C1-120 ^oC/C2-50 ^oC). Experimental data are mean values of three replicate runs, with error bars representing corresponding standard deviations of the replicate experimental runs.

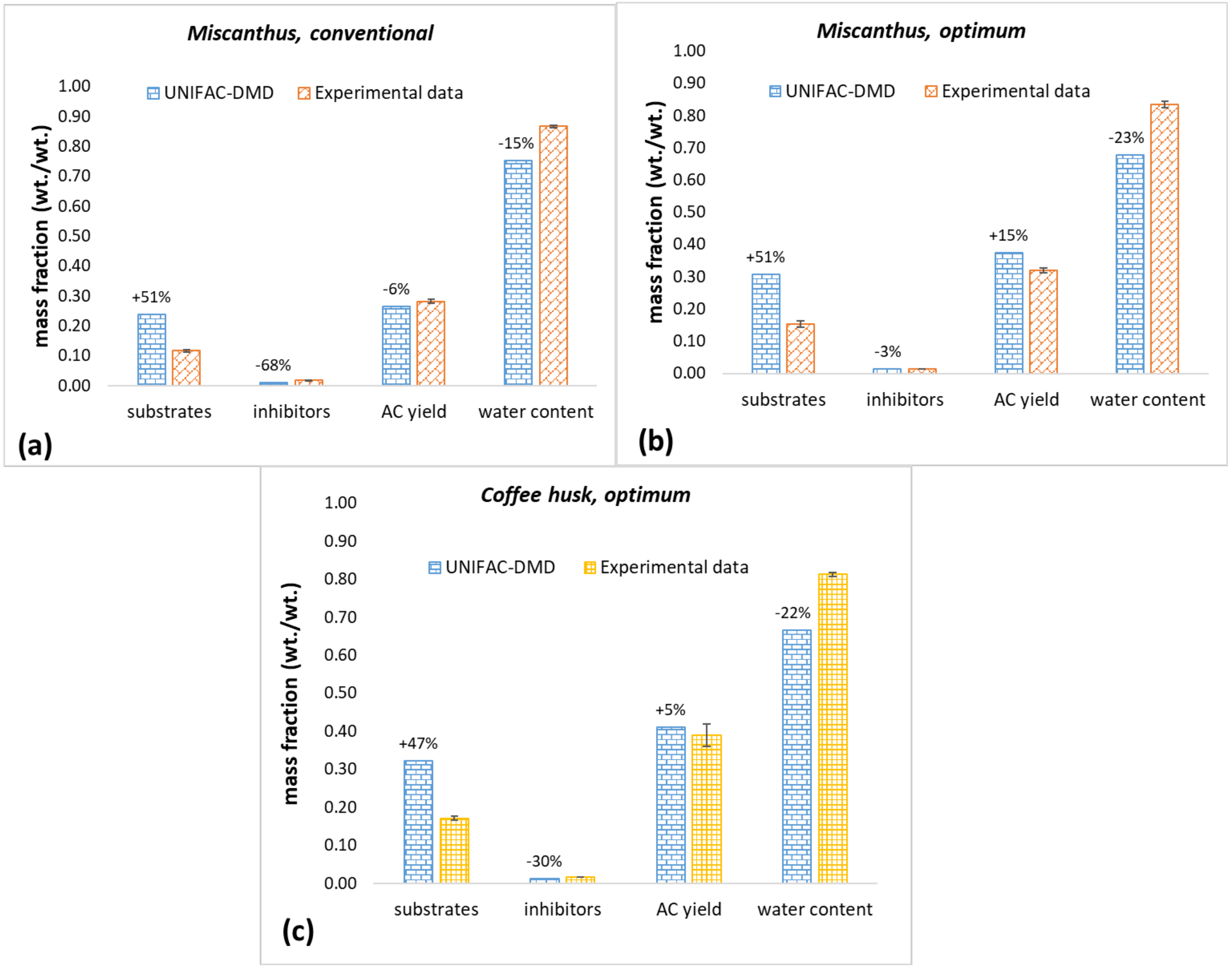

Fig. 6. Comparison of theoretical UNIFAC-DMD models for investigated parameters with experimental validations on PDU showing percentage deviations from experimental data: (a) comparisons at conventional condensation temperatures (C1-90 ^{o}C/C2-15 ^{o}C) for miscanthus; (b) comparisons at optimum condensation temperatures (C1-120 ^{o}C/C2-50 ^{o}C) for miscanthus; (c) comparisons at optimum condensation temperatures (C1-120 ^{o}C/C2-50 ^{o}C) for coffee husk. Experimental data are mean values of three replicate runs, with error bars representing corresponding standard deviations of the replicate experimental runs.

For wheat straw, except for the significant deviations of model data from experimental data observed for inhibitory compounds, prediction with the theoretical model essentially agrees with experimental validations on the PDU (Fig. 5). Models were even better predicted at conventional condensation temperatures (C1-90 ^{o}C/C2-15 ^{o}C), with percentage deviations of only 1% (under-prediction), 8% (under-prediction) and 14% (over-prediction) observed for the parameters: AC water content, AC yield and mass fraction of substrates, respectively (Fig. 5a). Similar trends were observed at optimum condensation temperatures (C1-120 ^{o}C/C2-50 ^{o}C) except that deviations at this temperature conditions (for all parameters bar inhibitors) were comparatively higher (Fig. 5b). With G^{E} models like the UNIFAC-DMD being only valid to upper limit temperatures of 120 ^{o}C [52], the comparatively higher deviations of model predictions observed at optimum condensation temperatures is of no surprise. The trends were no different for the case of *miscanthus* and coffee husk biomass feedstocks, where model predictions largely agree with experimental data (Fig. 6).

For all three biomass feedstocks, at all temperature combinations investigated, mass fractions of substrates and inhibitors tend to be the parameters with the strongest deviations. Most especially for inhibitors, even more significant under-prediction of experimental data was observed at both conventional and optimum operating temperature conditions. This was attributed to their comparatively low concentrations relative to the overall amount of AC. One known limitation of the UNIFAC-DMD model is its inability to accurately handle the infinite dilution of hydrocarbons in water [56]. With the significantly low concentrations of these organic compounds in AC, the much stronger deviations observed are obvious. The deviations were also blamed on the effects of uncertainties of the pure component vapour pressure data for some of the compounds. Most especially with the compounds estimated using the Extended Antoine equation (arising due to lack of experimental data), some associated uncertainties are definite. Overall, the UNIFAC-DMD thermodynamic model to a greater extent predicted the VLE behaviour of fast pyrolysis vapours although its limitations in handling highly dilute concentrations of the organic compounds became evident. More complex group contribution models like the Group Contribution Associating Equation of State (GCA-EoS) can potentially lead to a better prediction of these phase equilibria and should be considered in future studies.

*3.2.2 Assessment of experimental data of the secondary parameters, "P/I" and "P/I * Yield of AC" with model predictions*

The experimental data of the parameters, "*P/I*" and "*P/I * Yield of AC*" at optimum condensation temperature conditions (C1-120 ^{o}C/C2-50 ^{o}C) were compared with conventional condensation temperature conditions (C1-90 ^{o}C/C2-15 ^{o}C). Again, as per experimental data available, the assessment was primarily conducted for wheat straw and *miscanthus* biomass feedstocks. Yet again, experimental data were compared with model predictions.

In the assessment of "*P/I * Yield of AC*" for wheat straw and *miscanthus* biomass feedstocks, experimental data subsequently ascertained the fact that the optimum condensation temperature conditions was very suitable for producing more substrate compounds over inhibitors at an optimal recovery of AC. Experimental data recorded for this parameter increased by about thrice (wheat straw) and twice (*miscanthus*) as temperature increased from conventional to optimum conditions (Table 3). It is important to note that this parameter is a secondary computation of different terms and errors associated with each of the terms led to the weighty percentage deviations (within the ranges of +54 and +69%) of corresponding model-predicted values. Regardless of the weighty deviations of model predictions from experimental values, the trends observed as temperature conditions increased from conventional to optimised conditions were quite consistent.

Similar observations were made for the assessment of experimental data of "*P/I*", where data (for wheat straw and *miscanthus*) recorded at optimum conditions were nearly twice those recorded at conventional conditions (Table 4). As observed for the case of "*P/I * Yield of AC*", weighty deviations of model-predicted data from experimental data were also witnessed for this case, which was again corroborated to the accumulation of errors associated with the individual terms that make up the parameter (i.e., weight percent of promoters, P and inhibitors, I).

Interestingly, *miscanthus* and coffee husk recorded higher experimental values of "*P/I*" and "*P/I * Yield of AC*" at optimum conditions than wheat straw. This suggests that *miscanthus* and coffee husk tend to be more promising sources of substrates recovery in AC as compared to wheat straw.

These deductions underpin the fact that a carefully controlled fractional condensation of pyrolysis vapours does have a significant impact on the distribution of substrates and inhibitors in pyrolysis condensates. Similar pronouncements to this were made by Liaw et al. [33] when they investigated the effects of temperature variations on the first condensation unit (at a fixed temperature of the second) on the yield of AC and product distribution of compounds in AC from the fast pyrolysis of Douglas Fir Wood. They also reported increased production of substrates and AC yield at the expense of inhibitory compounds at high temperatures of C1. Their study, however, did not take into consideration the simultaneous variations of temperatures of both condensation units.

Table 3. Comparison of experimental data of the parameter, “*P/I * Yield of AC*” at optimum (C1-120 ^{o}C/C2-50 ^{o}C) with conventional (C1-90 ^{o}C/C2-15 ^{o}C) condensation temperatures and their correlation with model predictions for *all three biomass feedstocks.*

C1/C2 temperature combinations (^{o}C)	Wheat Straw			*Miscanthus*			Coffee Husk		
	P/I * Yield of AC (exp.)	Model prediction	PD (%)	P/I * Yield of AC (exp.)	Model prediction	PD (%)	P/I * Yield of AC (exp.)	Model prediction	PD (%)
120/50	2.61 (±0.00)	7.01	+63	3.53 (±0.20)	8.51	+59	4.03 (±0.33)	10.42	+61
90/15	1.15 (±0.03)	2.49	+54	1.92 (±0.21)	6.19	+69	N/A	7.74	N/A

*exp.-experimental data; PD-percent deviation of model prediction from experimental data; N/A-no experimental data available.

Table 4. *Comparison of experimental data of the parameter, “P/I” at optimum (C1-120 ^{o}C/C2-50 ^{o}C) with conventional (C1-90 ^{o}C/C2-15 ^{o}C) condensation temperatures and their correlation with model predictions for all three biomass feedstocks.*

C1/C2 Temperature combinations (^{o}C)	Wheat Straw			*Miscanthus*			Coffee Husk		
	P/I (exp.)	Model prediction	PD (%)	P/I (exp.)	Model prediction	PD (%)	P/I (exp.)	Model prediction	PD (%)
120/50	7.58 (±0.10)	19.70	+62	11.04 (±0.47)	23.11	+52	10.35 (±0.42)	25.37	+59
90/15	4.02 (±0.45)	8.74	+54	6.80 (±0.59)	23.26	+71	N/A	26.91	N/A

*exp.-experimental data; PD-percent deviation of model prediction from experimental data; N/A-no experimental data available.

4. Conclusions

The study demonstrated that fractional condensation of biomass fast pyrolysis vapours can be adjusted to optimise the composition of low-temperature, aqueous pyrolysis condensates (AC) to be used as substrates for microbial cultivation. For temperature ranges investigated, combinations of 120 ^{o}C and 50 ^{o}C on the first and second staged condensers, respectively were found to be the most suitable conditions for which recovery of substrates and AC product yield were maximised. As maximising the yield of AC lowers that of the main pyrolysis product, the organic-rich condensate, future work must lay in the inclusion of techno-economic data such that the concept is still economically viable.

Acknowledgements

This work was supported by the German Federal Ministry of Education and Research (BMBF) [grant number 031B0673A].

Supporting Information:

Additional selection procedure of surrogate compounds, unprocessed central composite Design (CCD) data and GC-MS analyses of all organic-rich and aqueous condensates (PDF).

References

[1] A. Tumbalam Gooty, D. Li, C. Briens, F. Berruti, Fractional condensation of bio-oil vapors produced from birch bark pyrolysis, Sep. Purif. Technol. 124 (2014) 81–88. https://doi.org/10.1016/j.seppur.2014.01.003.

[2] S. Ma, L. Zhang, L. Zhu, X. Zhu, Preparation of multipurpose bio-oil from rice husk by pyrolysis and fractional condensation, J. Anal. Appl. Pyrolysis. 131 (2018) 113–119.

https://doi.org/10.1016/j.jaap.2018.02.017.

[3] S. Wang, G. Dai, H. Yang, Z. Luo, Lignocellulosic biomass pyrolysis mechanism: A state-of-the-art review, Prog. Energy Combust. Sci. 62 (2017) 33–86. https://doi.org/10.1016/j.pecs.2017.05.004.

[4] S. Papari, K. Hawboldt, A review on condensing system for biomass pyrolysis process, Fuel Process. Technol. 180 (2018) 1–13. https://doi.org/10.1016/j.fuproc.2018.08.001.

[5] A.V. Bridgwater, D. Meier, D. Radlein, An overview of fast pyrolysis of biomass, Org. Geochem. 30 (1999) 1479–1493. https://doi.org/10.1016/S0146-6380(99)00120-5.

[6] D. Meier, B. Van De Beld, A. V. Bridgwater, D.C. Elliott, A. Oasmaa, F. Preto, State-of-the-art of fast pyrolysis in IEA bioenergy member countries, Renew. Sustain. Energy Rev. 20 (2013) 619–641. https://doi.org/10.1016/j.rser.2012.11.061.

[7] F.A. Sánchez, Y. Ille, N. Dahmen, S. Pereda, GCA-EOS extension to mixtures of phenol ethers and derivatives with hydrocarbons and water, Fluid Phase Equilib. 490 (2019) 13–21. https://doi.org/10.1016/j.fluid.2019.02.017.

[8] H. Sui, H. Yang, J. Shao, X. Wang, Y. Li, H. Chen, Fractional condensation of multicomponent vapors from pyrolysis of cotton stalk, Energy and Fuels. 28 (2014) 5095–5102. https://doi.org/10.1021/ef5006012.

[9] T. Schulzke, S. Conrad, J. Westermeyer, Fractionation of flash pyrolysis condensates by staged condensation, Biomass and Bioenergy. 95 (2016) 287–295. https://doi.org/10.1016/j.biombioe.2016.05.022.

[10] A.N. Huang, C.P. Hsu, B.R. Hou, H.P. Kuo, Production and separation of rice husk pyrolysis bio-oils from a fractional distillation column connected fluidized bed reactor, Powder Technol. 323 (2018) 588–593. https://doi.org/10.1016/j.powtec.2016.03.052.

[11] M. Chai, Y. He, Nishu, C. Sun, R. Liu, Effect of fractional condensers on characteristics, compounds distribution and phenols selection of bio-oil from pine sawdust fast pyrolysis, J. Energy Inst. (2019) 1–11. https://doi.org/10.1016/j.joei.2019.05.001.

[12] F.-X. Collard, M. Carrier, J.F. Gorgens, Fractionation of Lignocellulosic Material With Pyrolysis Processing, in: S.I. Mussatto (Ed.), Biomass Fractionation Technol. a

Lignocellul. Feed. Based Biorefinery, Elsevier Inc, 2016: pp. 81–101. https://doi.org/10.1016/C2014-0-01890-4.

[13] Y. Ille, F. Kröhl, A. Velez, A. Funke, S. Pereda, K. Schaber, N. Dahmen, Activity of water in pyrolysis oil—Experiments and modelling, J. Anal. Appl. Pyrolysis. 135 (2018) 260–270. https://doi.org/10.1016/j.jaap.2018.08.027.

[14] S. Papari, K. Hawboldt, P. Fransham, Study of selective condensation for woody biomass pyrolysis oil vapours, Fuel. 245 (2019) 233–239. https://doi.org/10.1016/j.fuel.2019.02.055.

[15] A.S. Pollard, M.R. Rover, R.C. Brown, Characterization of bio-oil recovered as stage fractions with unique chemical and physical properties, J. Anal. Appl. Pyrolysis. 93 (2012) 129–138. https://doi.org/10.1016/j.jaap.2011.10.007.

[16] B. Sukhbaatar, Q. Li, C. Wan, F. Yu, E.B. Hassan, P. Steele, Inhibitors removal from bio-oil aqueous fraction for increased ethanol production, Bioresour. Technol. 161 (2014) 379–384. https://doi.org/10.1016/j.biortech.2014.03.051.

[17] T.P. Vispute, G.W. Huber, Production of hydrogen, alkanes and polyols by aqueous phase processing of wood-derived pyrolysis oils, Green Chem. 11 (2009) 1433–1445. https://doi.org/10.1039/b912522c.

[18] S. Arnold, K. Moss, N. Dahmen, M. Henkel, R. Hausmann, Pretreatment strategies for microbial valorization of bio-oil fractions produced by fast pyrolysis of ash-rich lignocellulosic biomass, GCB Bioenergy. 11 (2019) 181–190. https://doi.org/10.1111/gcbb.12544.

[19] S. Dörsam, J. Kirchhoff, M. Bigalke, N. Dahmen, C. Syldatk, K. Ochsenreither, Evaluation of pyrolysis oil as carbon source for fungal fermentation, Front. Microbiol. 7 (2016) 1–11. https://doi.org/10.3389/fmicb.2016.02059.

[20] J. Lian, M. Garcia-Perez, R. Coates, H. Wu, S. Chen, Yeast fermentation of carboxylic acids obtained from pyrolytic aqueous phases for lipid production, Bioresour. Technol. 118 (2012) 177–186. https://doi.org/10.1016/j.biortech.2012.05.010.

[21] M.R. Rover, P.A. Johnston, L.E. Whitmer, R.G. Smith, R.C. Brown, The effect of pyrolysis temperature on recovery of bio-oil as distinctive stage fractions, J. Anal.

Appl. Pyrolysis. 105 (2014) 262–268. https://doi.org/10.1016/j.jaap.2013.11.012.

[22] A.C. Johansson, K. Iisa, L. Sandström, H. Ben, H. Pilath, S. Deutch, H. Wiinikka, O.G.W. Öhrman, Fractional condensation of pyrolysis vapors produced from Nordic feedstocks in cyclone pyrolysis, J. Anal. Appl. Pyrolysis. 123 (2017) 244–254. https://doi.org/10.1016/j.jaap.2016.11.020.

[23] Y. Elkasabi, C.A. Mullen, A.A. Boateng, Distillation and isolation of commodity chemicals from bio-oil made by tail-gas reactive pyrolysis, ACS Sustain. Chem. Eng. 2 (2014) 2042–2052. https://doi.org/10.1021/sc5002879.

[24] A. Niebel, A. Funke, C. Pfitzer, N. Dahmen, N. Weih, D. Richter, B. Zimmerlin, Fast Pyrolysis of Wheat Straw - Improvements of Operational Stability in 10 Years of Bioliq Pilot Plant Operation, Energy and Fuels. 35 (2021) 11333–11345. https://doi.org/10.1021/acs.energyfuels.1c00851.

[25] A. Funke, M. Tomasi Morgano, N. Dahmen, H. Leibold, Experimental comparison of two bench scale units for fast and intermediate pyrolysis, J. Anal. Appl. Pyrolysis. 124 (2017) 504–514. https://doi.org/10.1016/j.jaap.2016.12.033.

[26] S. Arnold, T. Tews, M. Kiefer, M. Henkel, R. Hausmann, Evaluation of small organic acids present in fast pyrolysis bio-oil from lignocellulose as feedstocks for bacterial bioconversion, GCB Bioenergy. 11 (2019) 1159–1172. https://doi.org/10.1111/gcbb.12623.

[27] L.N. Jayakody, C.W. Johnson, J.M. Whitham, R.J. Giannone, B.A. Black, N.S. Cleveland, D.M. Klingeman, W.E. Michener, J.L. Olstad, D.R. Vardon, R.C. Brown, S.D. Brown, R.L. Hettich, A.M. Guss, G.T. Beckham, Thermochemical wastewater valorization: Via enhanced microbial toxicity tolerance, Energy Environ. Sci. 11 (2018) 1625–1638. https://doi.org/10.1039/c8ee00460a.

[28] B.A. Black, W.E. Michener, K.J. Ramirez, M.J. Biddy, B.C. Knott, M.W. Jarvis, J. Olstad, O.D. Mante, D.C. Dayton, G.T. Beckham, Aqueous Stream Characterization from Biomass Fast Pyrolysis and Catalytic Fast Pyrolysis, ACS Sustain. Chem. Eng. 4 (2016) 6815–6827. https://doi.org/10.1021/acssuschemeng.6b01766.

[29] H. Zhou, R.C. Brown, Z. Wen, Anaerobic digestion of aqueous phase from pyrolysis of

biomass: Reducing toxicity and improving microbial tolerance, Bioresour. Technol. 292 (2019) 121976. https://doi.org/10.1016/j.biortech.2019.121976.

[30] C. Wen, C.M. Moreira, L. Rehmann, F. Berruti, Feasibility of anaerobic digestion as a treatment for the aqueous pyrolysis condensate (APC) of birch bark, Bioresour. Technol. 307 (2020) 123199. https://doi.org/10.1016/j.biortech.2020.123199.

[31] T. Nicoleit, N. Dahmen, J. Sauer, Production and Storage of Gasifiable Slurries Based on Flash-Pyrolyzed Straw, Energy Technol. 4 (2016) 221–229. https://doi.org/10.1002/ente.201500273.

[32] N. Dahmen, J. Abeln, M. Eberhard, T. Kolb, H. Leibold, J. Sauer, D. Stapf, B. Zimmerlin, The bioliq process for producing synthetic transportation fuels, Wiley Interdiscip. Rev. Energy Environ. 6 (2017). https://doi.org/10.1002/wene.236.

[33] S.S. Liaw, V.H. Perez, R.J.M. Westerhof, G.F. David, C. Frear, M. Garcia-Perez, Biomethane Production from Pyrolytic Aqueous Phase: Biomass Acid Washing and Condensation Temperature Effect on the Bio-oil and Aqueous Phase Composition, Bioenergy Res. 13 (2020) 878–886. https://doi.org/10.1007/s12155-020-10100-3.

[34] D. Fabbri, C. Torri, Linking pyrolysis and anaerobic digestion (Py-AD) for the conversion of lignocellulosic biomass, Curr. Opin. Biotechnol. 38 (2016) 167–173. https://doi.org/10.1016/j.copbio.2016.02.004.

[35] C. Kubisch, K. Ochsenreither, Detoxification of a pyrolytic aqueous condensate from wheat straw for utilization as substrate in Aspergillus oryzae DSM 1863 cultivations, Biotechnol. Biofuels Bioprod. 15 (2022) 1–21. https://doi.org/10.1186/s13068-022-02115-z.

[36] C. Torri, D. Fabbri, Biochar enables anaerobic digestion of aqueous phase from intermediate pyrolysis of biomass, Bioresour. Technol. 172 (2014) 335–341. https://doi.org/10.1016/j.biortech.2014.09.021.

[37] Z. Chi, M. Rover, E. Jun, M. Deaton, P. Johnston, R.C. Brown, Z. Wen, L.R. Jarboe, Overliming detoxification of pyrolytic sugar syrup for direct fermentation of levoglucosan to ethanol, Bioresour. Technol. 150 (2013) 220–227. https://doi.org/10.1016/j.biortech.2013.09.138.

[38] X. Zhao, K. Davis, R. Brown, L. Jarboe, Z. Wen, Alkaline treatment for detoxification of acetic acid-rich pyrolytic bio-oil for microalgae fermentation: Effects of alkaline species and the detoxification mechanisms, Biomass and Bioenergy. 80 (2015) 203–212. https://doi.org/10.1016/j.biombioe.2015.05.007.

[39] J.K.S. Chan, S.J.B. Duff, Methods for mitigation of bio-oil extract toxicity, Bioresour. Technol. 101 (2010) 3755–3759. https://doi.org/10.1016/j.biortech.2009.12.054.

[40] Y. Ille, F.A. Sánchez, N. Dahmen, S. Pereda, Multiphase Equilibria Modeling of Fast Pyrolysis Bio-Oils. Group Contribution Associating Equation of State Extension to Lignin Monomers and Derivatives, Ind. Eng. Chem. Res. 58 (2019) 7318–7331. https://doi.org/10.1021/acs.iecr.9b00227.

[41] T.M. Soria, A.E. Andreatta, S. Pereda, S.B. Bottini, Thermodynamic modeling of phase equilibria in biorefineries, Fluid Phase Equilib. 302 (2011) 1–9. https://doi.org/10.1016/j.fluid.2010.10.029.

[42] R.J.M. Westerhof, D.W.F. Brilman, M. Garcia-Perez, Z. Wang, S.R.G. Oudenhoven, W.P.M. Van Swaaij, S.R.A. Kersten, Fractional condensation of biomass pyrolysis vapors, Energy and Fuels. 25 (2011) 1817–1829. https://doi.org/10.1021/ef2000322.

[43] R.J.M. Westerhof, N.J.M. Kuipers, S.R.A. Kersten, W.P.M. Van Swaaij, Controlling the water content of biomass fast pyrolysis oil, Ind. Eng. Chem. Res. 46 (2007) 9238–9247. https://doi.org/10.1021/ie070684k.

[44] E.C. Carlson, Don’t Gamble With Physical Properties For Simulations, Chem. Eng. Prog. (1996) 35–46. http://www.cchem.berkeley.edu/cbe150b/docs/VLE/Guidelines.pdf.

[45] D. Constantinescu, J. Gmehling, Further development of modified UNIFAC (Dortmund): Revision and extension 6, J. Chem. Eng. Data. 61 (2016) 2738–2748. https://doi.org/10.1021/acs.jced.6b00136.

[46] L. V. Jasperson, R.J. McDougal, V. Diky, E. Paulechka, R.D. Chirico, K. Kroenlein, K. Iisa, A. Dutta, Liquid-liquid equilibrium measurements for model systems related to catalytic fast pyrolysis of biomass, J. Chem. Eng. Data. 62 (2016) 243–252. https://doi.org/10.1021/acs.jced.6b00625.

[47] C. Pfitzer, N. Dahmen, N. Tröger, F. Weirich, J. Sauer, A. Günther, M. Müller-Hagedorn,

Fast Pyrolysis of Wheat Straw in the Bioliq Pilot Plant, Energy and Fuels. 30 (2016) 8047–8054. https://doi.org/10.1021/acs.energyfuels.6b01412.

[48] Dortmund Data Bank, (n.d.). http://www.ddbst.de/unifac-consortium.html (accessed April 29, 2020).

[49] L.A. Forero G., J.A. Velásquez J., Wagner liquid-vapour pressure equation constants from a simple methodology, J. Chem. Thermodyn. 43 (2011) 1235–1251. https://doi.org/10.1016/j.jct.2011.03.011.

[50] T. Nichols, V. Utgikar, Wagner equation predicting entire curve for pure fluids from limited VLE data: Critical point & four Antoine analytic points, Fluid Phase Equilib. 460 (2018) 1–16. https://doi.org/10.1016/j.fluid.2017.12.022.

[51] VDI Heat Atlas. Second edition, Springer-Verlag Berlin Heidelberg, 2010. Ed. Verein Deutscher Ingenieure VDI-Gesellschaft Verfahrenstechnik und Chemieingenieurwesen (GVC). https://doi: 10.1007/978-3-540-77877-6.

[52] Stark, Y. H. (2020). Modellierung der Kondensation von Pyrolysedämpfen unter Berücksichtigung der Aerosolbildung (Publication No. ISBN: 978-3-8439-4483-0) [Doctoral dissertation, Karlsruher Institut für Technologie (KIT)]. https://primo.bibliothek.kit.edu/permalink/f/coi3a3/KITSRC172512288X.

[53] A. Funke, D. Richter, A. Niebel, N. Dahmen, J. Sauer, Fast pyrolysis of biomass residues in a twin-screw mixing reactor, J. Vis. Exp. 2016 (2016) 1–8. https://doi.org/10.3791/54395.

[54] F.G. Fonseca, A. Funke, A. Niebel, A.P. Soares Dias, N. Dahmen, Moisture content as a design and operational parameter for fast pyrolysis, J. Anal. Appl. Pyrolysis. 139 (2019) 73–86. https://doi.org/10.1016/j.jaap.2019.01.012.

[55] N. Charon, J. Ponthus, D. Espinat, F. Broust, G. Volle, J. Valette, D. Meier, Multi-technique characterization of fast pyrolysis oils, J. Anal. Appl. Pyrolysis. 116 (2015) 18–26. https://doi.org/10.1016/j.jaap.2015.10.012.

[56] J. Gmehling, B. Kolbe, M. Kleiber, J. Rarey, Chemical Thermodynamics for Process Simulation, Wiley-VCH Verlag GmbH & Co. KGaA, Boschstr. 12, 69469 Weinheim, Germany All, 2019.

TOC Graphic

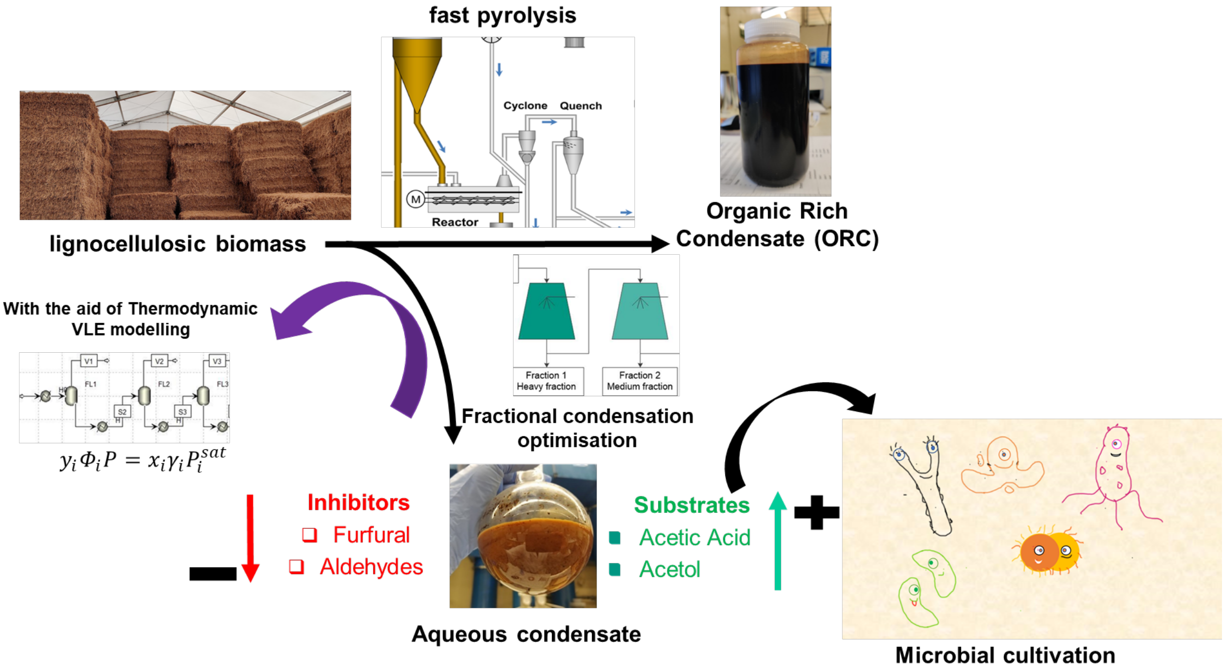
fast pyrolysis
Cyclone
Quench
M
Reactor
Organic Rich Condensate (ORC)
lignocellulosic biomass
With the aid of Thermodynamic VLE modelling
V1
V2
V3
FL1
FL2
FL3
S2
S3
$y_i \Phi_i P = x_i \gamma_i P_i^{sat}$
Fraction 1 Heavy fraction
Fraction 2 Medium fraction
Fractional condensation optimisation
Inhibitors
❑ Furfural
❑ Aldehydes
Substrates
■ Acetic Acid
■ Acetol
Aqueous condensate
Microbial cultivation